

# Analysis of structural patterns in the brain with the complex network approach

Vladimir A. Maksimenko<sup>a,b</sup>, Vladimir V. Makarov<sup>a,b</sup>, Alexander A. Kharchenko<sup>a,b</sup>,  
Alexey N. Pavlov<sup>a,c</sup>, Marina V. Khramova<sup>d</sup>, Alexey A. Koronovskii<sup>b,a</sup>,  
Alexander E. Hramov<sup>a,b</sup>

<sup>a</sup>Research and Educational Center “Nonlinear Dynamics of Complex Systems”,  
Saratov State Technical University, Polytechnicheskaya Str. 77, Saratov, 410054, Russia;

<sup>b</sup>Faculty of Nonlinear Processes, Saratov State University,  
Astrakhanskaya Str. 83, Saratov, 410012, Russia;

<sup>c</sup>Physics Dept., Saratov State University, Astrakhanskaya Str. 83, Saratov, 410012, Russia;

<sup>d</sup>Faculty of Computer Sciences and Information Technologies, Saratov State University,  
Astrakhanskaya Str. 83, Saratov, 410012, Russia

## ABSTRACT

In this paper we study mechanisms of the phase synchronization in a model network of Van der Pol oscillators and in the neural network of the brain by consideration of macroscopic parameters of these networks. As the macroscopic characteristics of the model network we consider a summary signal produced by oscillators. Similar to the model simulations, we study EEG signals reflecting the macroscopic dynamics of neural network. We show that the appearance of the phase synchronization leads to an increased peak in the wavelet spectrum related to the dynamics of synchronized oscillators. The observed correlation between the phase relations of individual elements and the macroscopic characteristics of the whole network provides a way to detect phase synchronization in the neural networks in the cases of normal and pathological activity.

**Keywords:** Complex network, electroencephalogram, continuous wavelet transform, oscillatory patterns, phase synchronization

## 1. INTRODUCTION

Studying brain dynamics and functions is one of the most widespread problems in the modern neuroscience, biophysics and medicine.<sup>1,2</sup> It is important in many areas of science dealing with the diagnostics and the treatment of brain disfunctions, the development of brain-computer interfaces, etc.<sup>3</sup> Interactions between a huge number of neurons lead to the appearance of local synchronous modes in different areas of the brain or, in some cases, to global synchronous states defining different types of cognitive functions.<sup>4</sup>

Currently, macroscopic signals reflecting the electrical activity of the neural network of the brain such as, e.g., an electroencephalogram (EEG)<sup>5</sup> or a magnetoencephalogram (MEG)<sup>6</sup> can be recorded with high resolution in both, space and time. Based on these data it becomes possible to identify specific patterns of neuron activity and to control the dynamics (e.g., to interrupt pathological activities during epileptic seizures<sup>7,8</sup>) or to translate patterns of neural activity into movement commands via special brain-computer interfaces<sup>3,9</sup>).

Typically, experimental analysis of neural networks is based on the macroscopic signals such as EEG or MEG that reflect cooperative dynamics of neurons in a certain part of the brain. Electrical activity of individual neurons can be studied using intracellular recordings providing a way to investigate very small groups of neural cells (typically, 2-3 neurons from a single recording). Experimental study of larger ensembles is a significantly more complicated problem. Analysis of the dynamics of neural network based on macroscopic signals and

Further author information: (Send correspondence to A.E. Hramov)  
A.E. Hramov: E-mail: hramovae@gmail.com, Telephone: +7 8452 51 42 94

revealing correlations between the dynamics of single nodes and the whole network are important problems in neurodynamics.<sup>10</sup>

In the given paper we study the dynamics of phases of individual nodes in the complex network of nonlinear oscillators involved into the global synchronous mode. We analyze a correspondence between distributions of the phase differences of interacting oscillators and the wavelet spectrum of the macroscopic dynamics of the network. As an example, we consider the network of  $N = 150$  Van der Pol oscillators.<sup>11-13</sup> The observed network is divided into subnetworks which are connected via the links between several elements. We analyze the development of the global synchronous regime in this model that involve elements from subnetworks. We discuss a possible application of the relations obtained with this model for the multichannel EEG recordings.

## 2. METHODS

In this study we deal with the macroscopic time-dependent characteristics of a model network. The analyzed macroscopic signal  $X(t)$  reflects a cooperation of the interacting nodes

$$X(t) = \sum_{i=1}^N x_i(t), \quad (1)$$

where  $x_i(t)$  are microscopic signals produced by each node. Introducing the phase  $\phi_i$  of each oscillator as

$$\phi_i = \arctan\left(\frac{\dot{x}_i}{x_i}\right) \quad (2)$$

let us consider distribution of the phase differences  $\Delta\phi = \phi_i - \phi_j, \forall i, j \in [1, N]$ .

Recent studies<sup>15</sup> revealed the possibility to detect structural clusters in adaptive networks based on wavelet analysis of macroscopic dynamics. Due to this, the signal  $X(t)$  is further analyzed with the continuous wavelet transform<sup>14</sup>

$$W(s, \tau) = \int_{-\infty}^{\infty} X(t)\varphi^*(s, \tau)dt, \quad (3)$$

where  $s$  is the time scale parameter, “\*” means the complex conjugation, and  $\varphi(s, \tau)$  is the wavelet function

$$\varphi(s, \tau) = \frac{1}{\sqrt{s}}\varphi_0\left(\frac{t-\tau}{s}\right). \quad (4)$$

Here,  $\varphi_0$  is the mother wavelet, and  $\tau$  is the translation parameter. According to earlier studies<sup>16-19</sup> we use the Morlet wavelet

$$\varphi_0(\eta) = \pi^{-\frac{1}{4}}e^{j\omega_0\eta}e^{-\frac{\eta^2}{2}} \quad (5)$$

with the central frequency  $\omega_0 = 2\pi$ . In this case, a relation between the Fourier frequency and the scale parameter can be written as  $f = 1/s$ . Aiming to characterize energy of the wavelet transform, we use the absolute value of the time averaged complex-valued function  $W(f)$ .

## 3. RESULTS

As the first example let us consider microscopic signals related to individual nodes as

$$x_i(t) = \cos(2\pi f^*t + \varphi_i) \quad (6)$$

Initially, the phases  $\varphi_i$  were normally distributed with the dispersion  $\sigma$ . Figure 1 illustrates the dependence of  $|W(f^*)|$  related to the frequency  $f^*$  for different values of the dispersion  $\sigma$  and different values of  $N$ . Reducing the amplitude of the peak in the wavelet spectrum with the dispersion of phase differences is observed, e.g., during the time scale synchronization<sup>20-22</sup> in complex networks.<sup>23</sup>

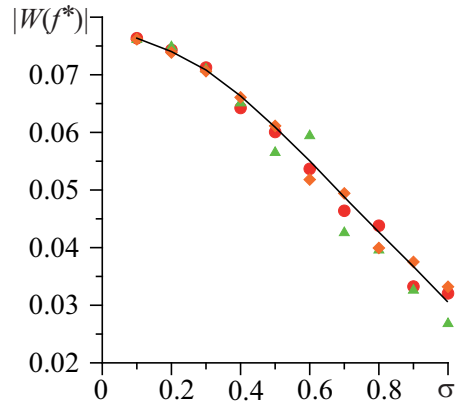


Figure 1. The dependence of  $|W(f^*)|$  of the signal (6) from the dispersion  $\sigma$  for different numbers of oscillators:  $N = 500$  (solid curve),  $N = 200$  (diamonds),  $N = 100$  (circles),  $N = 50$  (triangles).

As the second example consider the network of  $N = 150$  Van der Pol oscillators, where the dynamics of the each node is described by the differential equation

$$\frac{d^2 x_i}{dt^2} - \mu(1 - x_i^2) \frac{dx_i}{dt} + \omega_i^2 x_i = \epsilon \sum_{j=1}^N c_{ij} (x_i - x_j), \quad (7)$$

Here,  $i$  and  $j$  are the numbers of individual elements,  $\mu = 1.0$  is the control parameter,  $\epsilon$  is the coupling strength,  $\omega_i$  is the frequency of each oscillator. The coefficients  $c_{ij}$  determine links between the elements  $i$  and  $j$  ( $c_{ij} = 1.0$  for interacted oscillators, and  $c_{ij} = 0.0$  at the absence of coupling). In this study we use the condition of bidirectional links  $c_{ij} = c_{ji}$  and the condition of dissipativeness

$$c_{ii} = - \sum_{j=1}^N c_{ij}, \quad \forall j \neq i. \quad (8)$$

The analyzed network of Van der Pol oscillators is schematically illustrated in Fig. 2 and is divided into two subnetworks. Here, we consider subnetworks connected via the bidirectional links between seven elements. The subnetwork I consists of  $N_1 = 90$  elements, and subnetwork II consists of  $N_2 = 60$  elements.

In order to demonstrate the development of the global synchronization the frequencies  $\omega_i$  were uniformly distributed in the range  $[0.2, 0.4]$ , and the wavelet spectra of the macroscopic signal (1) were estimated for different values of the coupling strength. All oscillators demonstrate the synchronous mode with the increased coupling strength  $\epsilon$ . The corresponding wavelet spectra are shown in Fig. 2, *b* for several values of  $\epsilon$ :  $\epsilon = 0.3$  (curve 1),  $\epsilon = 0.5$  (curve 2),  $\epsilon = 0.7$  (curve 3), and  $\epsilon = 0.9$  (curve 4). There is a clearly expressed peak in the wavelet spectrum whose amplitude depends on  $\epsilon$ . Taking into account results of the first example, one can assume that this is caused by decreased dispersion of distribution of the phase differences, i.e. by the phase synchronization.

Aiming to analyze this phenomenon, consider distributions of the phase differences in the each subnetwork and plot the dependencies of their dispersion versus the coupling strength. The results are presented in Fig. 2, *c*. Curves 1 and 2 correspond to the subnetwork I and subnetwork II, respectively. One can see that the decreased dispersion of distribution of the phase differences is accompanied by the increased amplitude of the peak by analogy with the performed analysis of the signal (6).

Evolution of distributions of the phase differences in the analyzed subnetworks is illustrated in Fig. 3. Figures (*a, c, e, g*) correspond to elements of the subnetwork I and (*b, d, f, h*) – to elements of the subnetwork II. One can see a decrease of the dispersion of these distributions with the increased coupling strength.

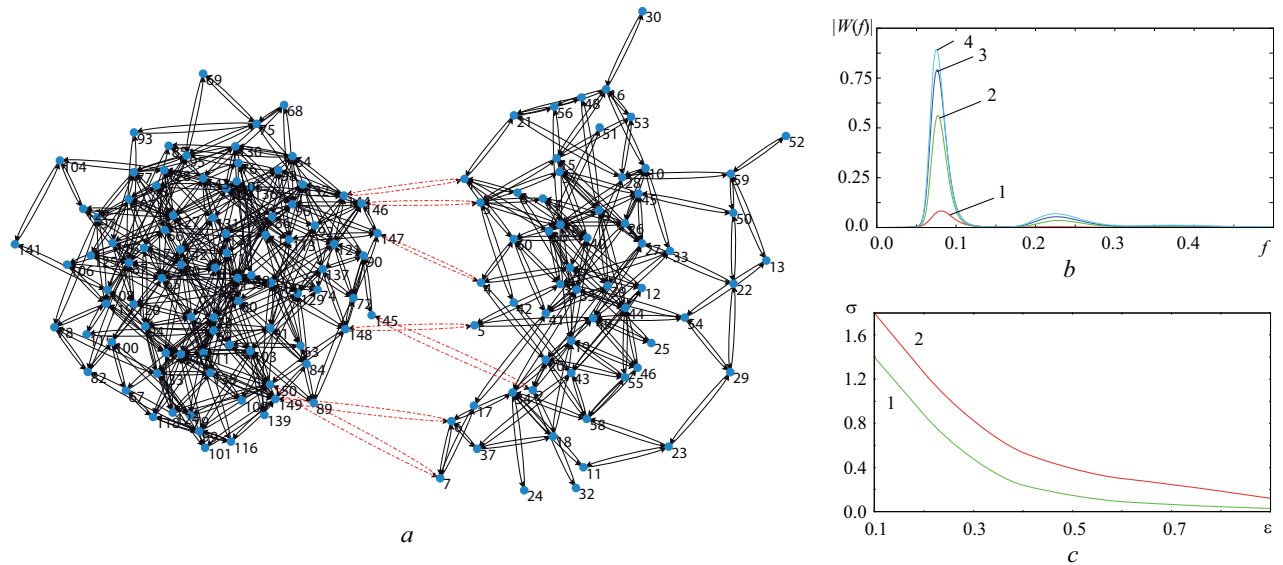


Figure 2. The analyzed network of Van der Pol oscillators (a), wavelet energy spectra of the macroscopic signal (1) for different values of  $\epsilon$  (b), and the dependencies of the dispersion of distributions of the phase differences versus the coupling strength for both subnetworks (1 and 2, respectively) (c).

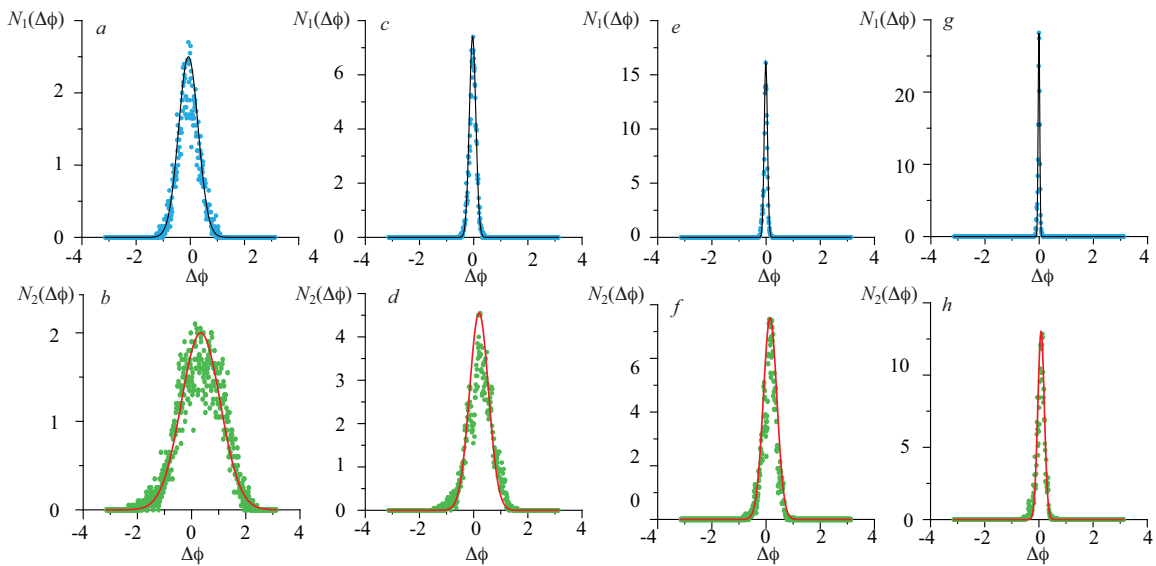


Figure 3. Distributions of the phase differences between Van der Pol oscillators for different values of the coupling strength  $\epsilon$ :  $\epsilon = 0.3$  (a,b),  $\epsilon = 0.5$  (c,d),  $\epsilon = 0.7$  (e,f),  $\epsilon = 0.9$  (g,h). Figures (a,c,e,g) correspond to elements of the subnetwork I and (b,d,f,h) are related to elements of the subnetwork II. Solid curves correspond to the Gaussian functions used for the approximation of the distributions.

Further we considered the network of Van der Pol oscillators (Fig. 2,a), where the frequencies are distributed in two different ranges related to each subnetwork. Here, we used non-overlapping ranges  $[0.1, 0.3]$  and  $[0.3, 0.5]$ . The results are shown in Fig. 4.

At small coupling strength, there are two different peaks in the wavelet spectrum of the macroscopic signal associated with the whole network (curve 1 in Fig. 4,a). These peaks are related to the dynamics of both subnetworks, where the oscillators are in the synchronous modes with certain frequencies. Increased  $\epsilon$  leads to the emergence of the global synchronization involving oscillators from the whole network (curve 4 in Fig. 4,a). In Fig. 4,b, the values of  $\sigma$  are shown for different values of the coupling strength. It is clearly seen, that for

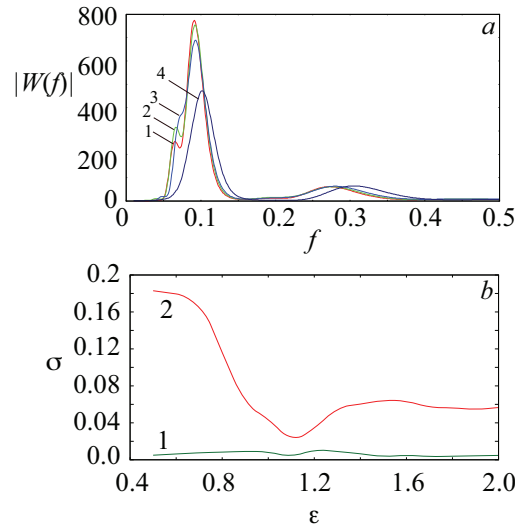


Figure 4. Wavelet energy spectra for the case when the frequencies of oscillators related to subnetworks I and II are distributed over different ranges (a). Four spectra are obtained for different values of the coupling strength  $\epsilon$ :  $\epsilon = 0.5$  (curve 1),  $\epsilon = 0.7$  (curve 2),  $\epsilon = 1.0$  (curve 3),  $\epsilon = 1.5$  (curve 4). (b) Dispersion  $\sigma$  of the phase distribution corresponding to subnetwork I (curve 1) and subnetwork II (curve 2) depending on the coupling strength  $\epsilon$ .

$\epsilon < 1.0$  the dispersion related to subnetwork II rapidly decreases while the dispersion of the phase differences in subnetwork I weakly increases. Such behaviour correlates with the evolution of wavelet spectra. According to Fig. 4,a the peak corresponding to subnetwork II grows while the peak corresponding to subnetwork I becomes lower. Figure 4,a also demonstrates that the observed peaks become merged that indicates the regime of the global synchronization. It is important to note that this regime is characterized by increased dispersion of distribution of the phase differences in both subnetworks. As the result, the corresponding spectral peak (curve 4 in Fig. 4,a) decreases.

#### 4. POSSIBLE APPLICATION OF THE PROPOSED APPROACH TO ANALYSIS OF NEURONAL NETWORK OF THE BRAIN

In this section we discuss the possibility of application of the obtained results to analyze neural network of the brain. For this purpose we shall use two signals of multichannel EEG taken from different regions of the rat's brain during the emergence of seizures of the absence epilepsy. EEGs were recorded in six male WAG/Rij rats (one year old, body weigh 320–360 g).<sup>24,25</sup> Experiments were performed in the laboratory of Biological Psychology, Donders Institute for Brain, Cognition and Behavior of Radboud University Nijmegen (Netherlands). The experiments were conducted in accordance with the legislations and regulations for animal care and were approved by the Ethical Committee on Animal Experimentation of the Radboud University Nijmegen. Distress and suffering of animals were kept to a minimum. Recording electrodes were implanted epidurally over the frontal cortex for the reason that SWDs and sleep spindles showed their amplitude maximum in this region. Ground and reference electrodes were placed over the two symmetrical sides of the cerebellum. Multichannel EEG recordings were made in freely moving rats continuously during a period of 2 h. EEG signals were fed into a multi-channel differential amplifier via a swivel contact, band-pass filtered between 0.5 and 100 Hz, digitized with 1024 samples/s/per channel (CODAS software).

Typical EEG signals containing spontaneous spike-wave discharges (but not pharmacologically induced seizures) are shown in Fig. 5. Spike-wave discharges are electroencephalographic hallmarks of generalized idiopathic epilepsies, such as the absence epilepsy and other syndromes. They can happen when synchronization in the neural network becomes too high (hyper-synchronization), or when cortical neurons express too strong excitation (hyper-excitation) in response to a thalamic input. So, there is considerable interest in the use of network approaches to study of synchronization of neural network before and during epileptic seizures.

In Fig 5, wavelet energy spectra of these signals are shown for the time moments  $t_1 = 120$  s (before spike-wave discharge) and  $t_2 = 125$  s (the onset of the seizure).

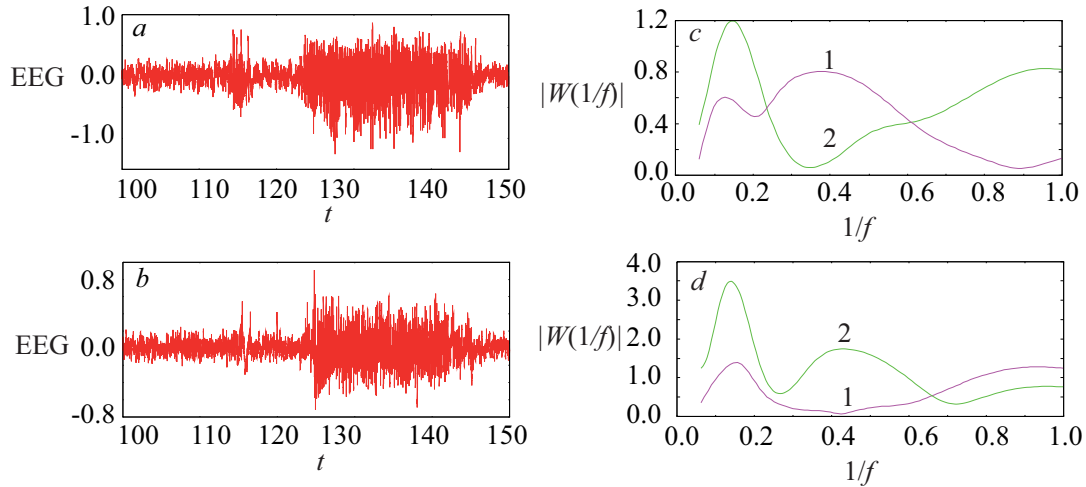


Figure 5. Multichannel EEG signals taken from different parts of the rat brain (*a,b*) and the wavelet energy spectra of these signals at the time moments  $t_1 = 120$  s and  $t_2 = 125$  s (*c,d*)

During the onset of epileptic activity the neurons in the considered areas of the brain demonstrate synchronous oscillations with the frequency  $f_{SWD} \approx 7$  Hz ( $s \approx 0.15$  s). This activity is observed in the wavelet spectra as the peak related to the corresponding time scale (or frequency) (Fig 5,*c*). The development of seizures is associated with increased strength of coupling between the areas of brain and, similar to the considered Van der Pol oscillators, indicates the emergence of the phase synchronization in neuron ensemble. This synchronization results in the increased spectral peaks in the wavelet spectra (Fig 5,*d*).

## 5. CONCLUSION

In this work we considered the emergence of synchronous modes in a network of Van der Pol oscillators with increased strength of coupling between individual oscillators. We showed a correspondence between the phases of single oscillators and the wavelet spectrum of the macroscopic signal, produced by the whole network. According to the obtained results, phase synchronization between network's elements leads to increased spectral peaks related to the synchronous regime. Increased wavelet energy was also demonstrated for EEG signals recorded from rat's brain during the onset of the epileptic seizure.

## ACKNOWLEDGMENTS

The authors express their sincere acknowledgments to Prof. Gilles van Luitelaar for providing experimental facilities and WAG/Rij rats in Donders Institute for Brain, Cognition and Behavior. This work has been supported by the Russian Foundation of Basic Research (grant 15-02-00624), Ministry of Education and Science of Russian Federation in the framework of the implementation of state assignment 3.23.2014/K (project SSTU-157) and within the basic part (project SSTU-141). A.E.H. also acknowledges support from the Ministry of Education and Science of Russian Federation in the framework of the providing researches (project 931 (project SSTU-146)).

## REFERENCES

- [1] Hagmann, P., Cammoun, L., Gigandet, X., Meuli, R., Honey, C. J., Wedeen, V. J., and Sporns, O., "Mapping the structural core of human cerebral cortex," *PLoS Biology* **6**, e159 (2008).
- [2] Valencia, M., Martinerie, J., Dupont, S., and Chavez, M., "Dynamic small-world behavior in functional brain networks unveiled by an event-related networks approach," *Phys. Rev. E* **77**(5), 050905 (2008).

- [3] Santhanam, G., Ryu, S. I., Yu, B. M., Afshar, A., and Shenoy, K. V., “A high-performance brain–computer interface,” *Nature Letters* **442**, 195–198 (2006).
- [4] Uhlhaas, P., Pipa, G., Lima, B., Melloni, L., Neuenschwander, S., Nikolic, D., and Singer, W., “Neural synchrony in cortical networks: history, concept and current status,” *Frontiers in Integrative Neuroscience* **3**, 17 (2009).
- [5] Ball, T., Kern, M., Mutschler, I., Aertsen, A., and Schulze-Bonhage, A., “Signal quality of simultaneously recorded invasive and non-invasive EEG,” *NeuroImage* **46**, 708–716 (2009).
- [6] Cohen, D., “Magnetoencephalography: evidence of magnetic fields produced by alpha-rhythm currents,” *Science* **161**, 784–786 (1968).
- [7] Beronyi, A., Belluscio, M., Mao, D., and Buzsáki, G., “Closed-loop control of epilepsy by transcranial electrical stimulation,” *Science* **337**, 735–737 (2012).
- [8] Ovchinnikov, A. A., Hramov, A. E., Luttjohann, A., Koronovskii, A. A., and Van Luijtelaar, E. L., “Method for diagnostics of characteristic patterns of observable time series and its real-time experimental implementation for neurophysiological signals,” *Technical Physics* **56**(1), 1–7 (2011).
- [9] Ovchinnikov, A. A., Luttjohann, A., Hramov, A. E., and Luijtelaar van, G., “An algorithm for real-time detection of spike-wave discharges in rodents,” *Journal of Neuroscience Methods* **194**, 172–178 (2010).
- [10] Makarov, V. V., Osipov, G. V., Maksimenko, V. A., and Kharchenko, A. A., “Synchronization of elements with different dimensions of their ensembles in a complex network,” *Technical Physics Letters* **41**, 69–75 (2015).
- [11] Balanov, A. G., Janson, N. B., Astakhov, V., and McClintock, P. V., “Role of saddle tori in the mutual synchronization of periodic oscillations,” *Phys. rev. E* **72**, 026214 (2005).
- [12] Hramov, A. E., Koronovskii, A. A., and Kurovskaya, M. K., “Two types of phase synchronization destruction,” *Phys. Rev. E* **75**(3), 036205 (2007).
- [13] Balanov, A. G., Janson, N. B., Postnov, D. E., and Sosnovtseva, O. V., [*Synchronization: from simple to complex*], Springer, Berlin, Heidelberg (2009).
- [14] Hramov, A. E., Koronovskii, A. A., Makarov, V. A., Pavlov, A. N., and Sitnikova, E. Y., [*Wavelets in Neuroscience*], Springer, Berlin, Heidelberg (2015).
- [15] Maksimenko, V. A., Makarov, V. V., Koronovskii, A. A., Hramov, A. E., and Moskalenko, O. I., “Analyzing the structure of a complex network on the basis of its macroscopic characteristics,” *Bulletin of the Russian Academy of Sciences. Physics* **78**, 1281–1284 (2014).
- [16] Sitnikova, E., Hramov, A. E., Koronovskii, A. A., and Luijtelaar, E. L., “Sleep spindles and spike-wave discharges in EEG: Their generic features, similarities and distinctions disclosed with fourier transform and continuous wavelet analysis,” *Journal of Neuroscience Methods* **180**, 304–316 (2009).
- [17] Pavlov, A. N., Hramov, A. E., Koronovskii, A. A., Sitnikova, Y. E., Makarov, V. A., and Ovchinnikov, A. A., “Wavelet analysis in neurodynamics,” *Physics-Uspekhi* **55**(9), 845–875 (2012).
- [18] Sitnikova, E., Hramov, A. E., Grubov, V., and Koronovsky, A. A., “Time-frequency characteristics and dynamics of sleep spindles in WAG/Rij rats with absence epilepsy,” *Brain Research* **1543**, 290–299 (2014).
- [19] Nazimov, A. I., Pavlov, A. N., Nazimova, A. A., Grubov, V. V., Koronovskii, A. A., Sitnikova, E., and Hramov, A. E., “Serial identification of EEG patterns using adaptive wavelet-based analysis,” *Eur. Phys. J. Special Topics* **222**, 2713–2722 (2013).
- [20] Hramov, A. E., Koronovskii, A. A., Kurovskaya, M. K., and Moskalenko, O. I., “Synchronization of spectral components and its regularities in chaotic dynamical systems,” *Phys. Rev. E* **71**(5), 056204 (2005).
- [21] Hramov, A. E. and Koronovskii, A. A., “An approach to chaotic synchronization,” *Chaos* **14**(3), 603–610 (2004).
- [22] Hramov, A. E., Koronovskii, A. A., Ponomarenko, V. I., and Prokhorov, M. D., “Detecting synchronization of self-sustained oscillators by external driving with varying frequency,” *Phys. Rev. E* **73**(2), 026208 (2006).
- [23] Moskalenko, O. I., Phrolov, N. S., Koronovskii, A. A., and Hramov, A. E., “Synchronization in the network of chaotic microwave oscillators,” *Eur. Phys. J. Special Topics* **222**, 2571–2582 (2013).
- [24] Coenen, A. M. and Luijtelaar van, E. L. M., “Genetic animal models for absence epilepsy: a review of the WAG/Rij strain of rats,” *Behav. Genet* **33**, 635–655 (2003).
- [25] Coenen, A. M. and Van Luijtelaar, E. L., “The WAG/Rij rat model for absence epilepsy: age and sex factors,” *Epilepsy Res.* **1**(5), 297–301 (1987).